

Discrete element simulation of localized deformation in stochastic distributed granular materials

WANG DengMing & ZHOU YouHe[†]

Key Laboratory of Mechanics on Western Disaster and Environment, Ministry of Education of China, Department of Mechanics, Lanzhou University, Lanzhou 730000, China

The deformation in granular material under loading conditions is a problem of great interest currently. In this paper, the micro-mechanism of the localized deformations in stochastically distributed granular materials is investigated based on the modified distinct element method under the plane strain conditions, and the influences of the confining pressure, the initial void ratio and the friction coefficient on the localized deformation and the stability of granular materials are also studied. It is concluded, based on the numerical simulation testing, that two crossed shear sliding planes may occur inside the granular assembly, and deformation patterns vary with the increasing of transverse strain. These conclusions are in good agreement with the present experimental results. By tangential velocity profiles along the direction normal to the two shear sliding planes, it can be found that there are two different shear deformation patterns: one is the fluid-like shear mode and the other is the solid-like shear mode. At last, the influences of various material parameters or factors on localized deformation features and patterns of granular materials are discussed in detail.

granular material, localized deformation, modified discrete element method

1 Introduction

Granular material is a collection of a large number of discrete particles which can move independently from one another and interact only at contact points. These discrete characteristics of granular material would result in many complex behaviors different from the common solid and fluid materials. In order to investigate these micro-mechanical and physical behaviors of granular material, much research work has been done in many application fields over the last decades. Within these research fields, the deformation in granular material under loading conditions is a

Received December 5, 2007; accepted April 16, 2008

doi: 10.1007/s11433-008-0132-4

[†]Corresponding author (email: zhoyuh@lzu.edu.cn)

Supported by the Key Project of the National Natural Science Foundation of China (Grant No. 10532040)

problem of great interest because it has many important industrial applied backgrounds, such as processing of groundwork in civil engineering, stability analysis of slope and human-built embankment, storage, transport and handling of grains and powders, design and maintenance of granular pavement^[1,2]. In many industries involving granular materials, the localized deformation is the major cause of the whole assembly's inefficiencies and failures which may often involve serious financial penalties. Over the last few decades, many investigations have been carried out to study the deformation of granular material, including experiments, theories and numerical simulations.

So far, many experiments have been done to reveal the deformation characteristic of granular material under different boundary and loading conditions^[3-5]. These experiments pay more attention to macro-deformation features of granular material, such as failure pattern, occurrence of shear band, and stress-strain relation. However, the micro-deformation mechanism leading to instabilities and failures of granular material has not been well understood yet. A primary reason is that it is a technical challenge to observe the micro-deformation processes taking place inside granular material^[3].

The theory analysis is a practical approach to investigating the deformation features of the dense granular material. This approach is based on the continuum mechanics model and the finite element method or other numerical schemes, and can solve many deformation problems under different boundaries or loading conditions^[6-8]. The constitutive equations play an important role in these continuum mechanics-based numerical processes. Most theoretical investigations on granular material focus on developing proper continuum constitutive equations, which distinguish granular material from other common materials. Though many scientists and engineers have devoted great efforts in this field, there is no theoretical model that is widely accepted for granular material at present^[7]. The major cause is that most of the constitutive equations cannot completely take account of the material's micro-structures and contact features between individual particles. However, the localized deformation in granular material is completely controlled by these micro-factors, so the results derived from the continuum mechanics-based numerical processes cannot exactly reflect the actual deformation patterns in granular material.

In order to satisfy the current engineering requirements, investigators pay more attention to the numerical simulations to solve the existing problems involving granular material^[5]. The discrete element method is a popular numerical simulation method to simulate the deformation of granular material, and many investigators have done some research work combining different problems. Under quasi-static loading conditions, Iwashita and Oda have concluded, based on the numerical simulation testing, that the basic micro-deformation mechanism ending up with the formation of shear bands is the generation of a column-like structure during the hardening process and its collapse in the softening process^[9,10]. Also, some research papers have shown that the rolling resistance in DEM simulations of granular material plays an important role^[9-11]. Hu et al. have studied the phenomenon of the strain localization in densely distributed metallic assemblies and analyzed the influences of Young's modulus, coefficient of friction, uniaxial yield stress, and the rolling resistance on the characteristics of shear bands^[12].

Although a lot of investigations have been done by experimental, theoretical and numerical simulation approaches on the localized deformation of granular material, there is still a lack of understanding for localized deformation of stochastic distributed granular material under durative loading conditions, i.e. how various external factors or materials parameters combine to influence

patterns and evolve features of the localized deformation. Based on the numerical simulation method, this paper analyzes the localized deformation features in granular material in which the distributions of diameter magnitude and position are stochastic under plain strain conditions, and investigates the influence of external factors or materials parameters on localized deformation features in granular material, such as initial void ratio, confining pressure and coefficient of friction.

2 Modified discrete element method

The discrete element method (DEM) proposed by Cundall is a promising numerical tool for simulating various problems involving granular material. The position of each particle in the system is obtained by integrating twice with respect to time in Newton's second law of motion^[13]. DEM is in fact a time-driven soft-particle method that allows two particles to interpenetrate so as to mimic particle deformation. Also it allows the relative motions between individual particles and does not need to satisfy displacement continuous conditions, so this method can efficiently simulate more complex mechanical characteristics of granular material, such as large deformation and nonlinearity.

2.1 Equations of motion

The calculations in DEM are performed using the Newton's second law of motion and the force-displacement law at the contact point. The governing equations of motion for particle i are^[14,15]

$$m_i \frac{d\mathbf{v}_i}{dt} = \sum \mathbf{F}_{ji}^c + \mathbf{F}_i, \quad (1)$$

$$I_i \frac{d\omega_i}{dt} = \sum (\mathbf{R}_i \times \mathbf{F}_{ji}^c + M_{ji}^o) + M_i, \quad (2)$$

where m_i and I_i are the particle mass and moment inertia, \mathbf{v}_i and ω_i are the particle translational and rotational velocity, \mathbf{F}_i and M_i are the non-contact forces and non-contact moments, \mathbf{F}_{ji}^c is the contact force of particle i due to particle j , \mathbf{R}_i is the vector directed from the center of particle i to the contact point, and M_{ji}^o is the rolling resistance moment between particle i and j due to the asymmetric normal stress in the contact plane.

2.2 Evaluation of contact forces

The interactions between two particles can be described using the relative distances between centers of the two particles, as shown in Figure 1. So the contact condition of the two particles i and j is simply given by

$$\delta_n = (R_i + R_j) - D_{ij} > 0, \quad (3)$$

where D_{ij} is the distance between centers of particles i and j with radius R_i and R_j , respectively. The contact force \mathbf{F}_{ji}^c between particles i and j , which can be decomposed into the normal contact force \mathbf{F}_{ji}^{cn} and the tangential contact force \mathbf{F}_{ji}^{cs} , is given by

$$\mathbf{F}_{ji}^c = \mathbf{F}_{ji}^{cn} + \mathbf{F}_{ji}^{cs} = F_{ji}^{cn} \mathbf{n}_{ji} + F_{ji}^{cs} \mathbf{s}_{ji}, \quad (4)$$

where \mathbf{n}_{ji} and \mathbf{s}_{ji} are the unit vectors of normal direction and tangential direction respectively at

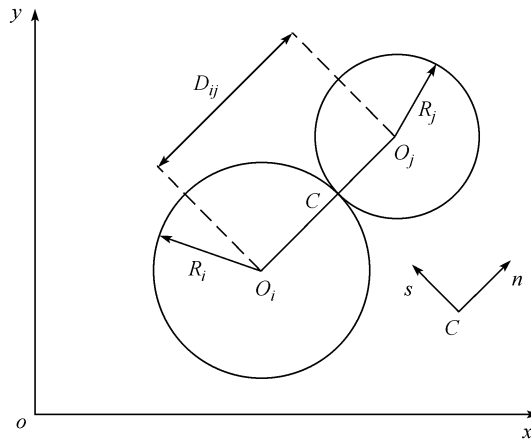


Figure 1 Interaction between two particles.

the contact plane between particles i and j . The normal force between the particles is modeled by a linear spring-dashpot model^[16,17]. The spring force provides an elastic restoration and the damping force dissipates the energy as the particles collide with neighboring particles or with the walls. So the normal contact force \mathbf{F}_{ji}^{cn} acting on particle i from particle j is given by

$$F_{ji}^{cn} = k_n \delta_n - c_n m_e (\mathbf{v}_r \cdot \mathbf{n}_{ij}), \quad (5)$$

where $m_e = (m_i m_j) / (m_i + m_j)$, m_e is the effective mass, k_n the normal elastic constant, c_n the normal dashpot coefficient, and \mathbf{v}_r the relative velocity vector between particles. The tangential contact force F_{ji}^{cn} acting on particle i from particle j is given by

$$F_{ji}^{cs} = -\text{sign}(\delta_s) \min(k_s |\delta_s|, \mu |F_{ji}^{cn}|) - c_s m_e (\mathbf{v}_r \cdot \mathbf{s}_{ij}), \quad (6)$$

where k_s is the tangential elastic constant, c_s the tangential dashpot coefficient, μ the friction coefficient, and δ_s the tangential displacement during the contact. When the magnitude of the sliding frictional force $\mu |F_{ji}^{cn}|$ exceeds the magnitude of tangential elastic force $k_s |\delta_s|$, the sliding frictional force becomes active and replaces the tangential elastic force.

2.3 Rolling resistance

It is assumed in the conventional DEM that particle rotations are controlled by the moments solely resulting from the tangential contact forces at particle contacts or suppressed to zero in the simulation. However, the current experiment and numerical simulation results show that the particle rotation, in particular, the rolling resistance, plays an important role in deformation characteristics of granular material^[9-11]. Generally, when a particle i contacts with another particle j , the initial contact point can gradually evolve to a finite contact area due to the particle deformation around the contact point. At the contact interface, if the tangential component of contact force is non-zero, the normal component of contact force will distribute asymmetrically about the centre of the contact interface as shown in Figure 2, resulting in a force couple known as the rolling resistance^[11]. So we can modify the discrete element method through the added rolling resistance so as to make the simulation results closer to the actual deformation of granular material.

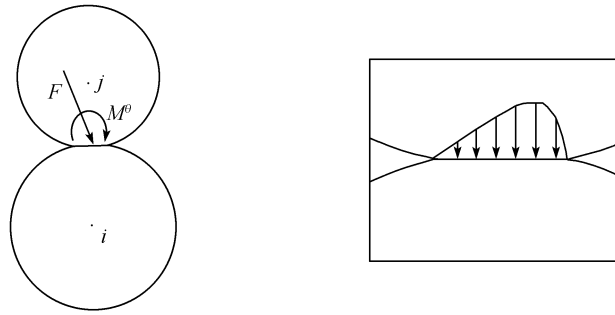


Figure 2 Sketch for rolling resistance at the contact interface.

In this paper, the common physical model of the rolling resistance between particles is modeled by the spring-dashpot model, in which each contact point is replaced by a set of torsion spring and dashpot. Similar to the Mohr-Coulomb criterion, the rolling resistance can be calculated by

$$\begin{cases} M_{\theta} = K_r \Delta\theta & K_r \Delta\theta < \eta F^n \\ M_{\theta} = \eta F^n = \alpha B F^n & \text{else} \end{cases} \quad (7)$$

where K_r is the stiffness of the torsion spring, $\Delta\theta$ the relative rotation between two particles, and η the rolling friction coefficient. It is shown that parameter η is related with the interface area of contact particles, so η can be decomposed into two components: the interface width B and the parameter α which depends on the distribution of contact force at the contact interface. Through the theoretical analysis^[11], the parameter α equals 1/3 approximately.

3 Numerical investigation

3.1 Numerical model

In order to investigate the localized deformation characteristics in granular material, it is necessary to put forward an appropriate numerical model. As shown in Figure 3, we consider a two-dimensional model containing numerous stochastic distributed discs under the plain strain conditions. The rectangle assembly is controlled by four boundaries: the bottom boundary is the fixed rigid platen, and the top boundary moves vertically down with a given speed as a loading platen. The left and right boundaries add a confining pressure to ensure the initial stability of granular material. When the transverse strain exceeds the limit value, the localized deformation will occur inside the granular material.

The granular assembly consists of about 4000 discs with stochastic distributed diameters and positions. The diameters of the whole granular material obey uniform distribution between 1–3 mm,

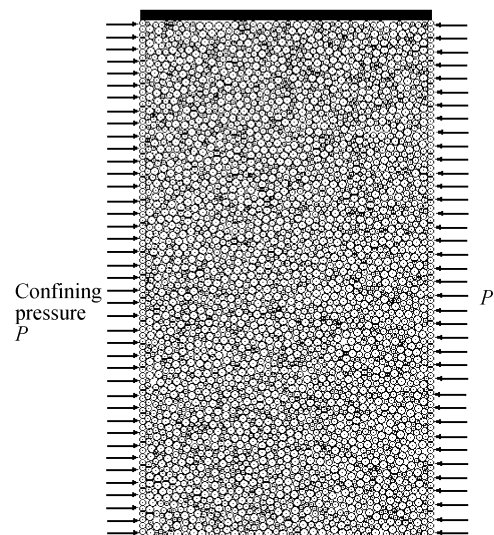


Figure 3 A physical model under plane strain conditions.

and D is the median particle diameter. We prepare the initial granular system by the gravitational deposited method that the particles with stochastic velocities in magnitudes and directions are randomly dropped into a rectangle container and tracing motions of particles until the final state is achieved. After compaction and relaxation of residual stresses^[18], an initial rectangular assembly under the plain strain conditions is prepared.

In this paper, the width and height of rectangular assembly are $l = 88$ mm and $h = 178$ mm, respectively. The model parameters in numerical simulation are given as follows^[16,17]: particle density $\rho = 2850$ kg/m³, friction coefficient between particles $\mu = 0.3$, friction coefficient between particle and loading plate $\mu_l = 0.35$, normal spring constant $k_n = 1.0 \times 10^7$ N/m, tangential spring constant $k_s = 2/3 \times K_n$, rolling spring constant $k_r = 1.3 \times 10^2$ N · m/rad, normal damping coefficient and tangential damping coefficient between particles are $c_n = 8.33 \times 10^{-2}$ N · s/m and $c_s = 8.33 \times 10^{-2}$ N · s/m, respectively, and coefficient of rolling damping $c_r = 1.0 \times 10^{-2}$ N · m · s/rad. The increment of time step $\Delta t = 10^{-6}$ s.

3.2 Characteristics of localized deformation

Different from the common solid materials, granular material under external loading conditions exhibits distinct features of localized deformation. Because the granular material also possesses some behaviors of the fluid materials, localized fluidities can take place inside granular material during durative loading and may gradually evolve into shear sliding planes. The moving velocities of the particle at the one side of shear plane are obviously greater than those at another side. Unlike the common annular shear or plane shear flows^[19], two crossed shear sliding planes can occur along the top of the granular assembly under the plane strain condition. The transverse strain is defined as follows:

$$\varepsilon = \frac{\Delta h}{h}, \quad (8)$$

where Δh is the transverse displacement of the top loading plate, and h is the initial height of granular assembly. Figure 4 shows velocity vectors of all particles at different transverse strain stages (median particle diameter $D = 2$ mm, confining pressure $\sigma_c = 15$ kPa, loading speed $v = 0.3$ m/s). The arrow's lengths are scaled relative to each other to show the magnitudes of individual

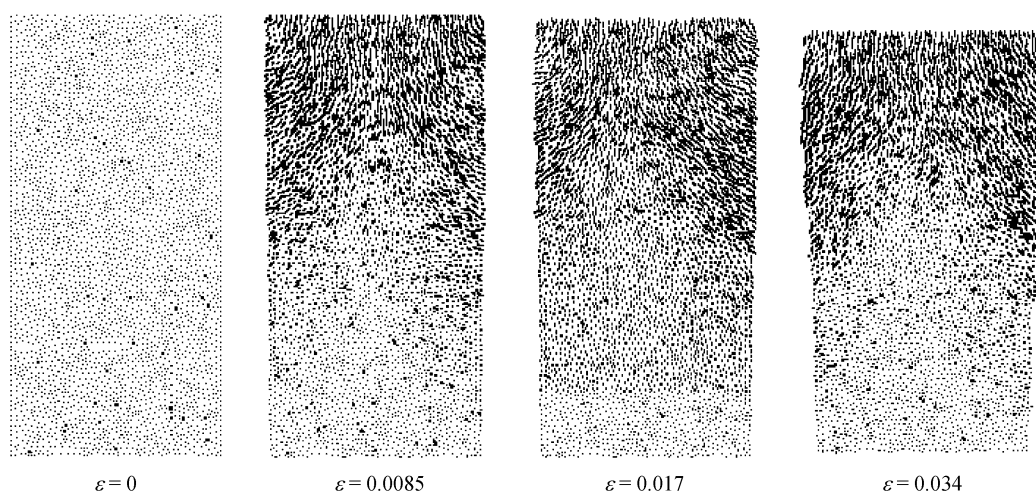


Figure 4 Velocity vectors of all particles at different transverse strain stages.

particle velocities. From the figure, we can see that deformations localized into narrow zones and two crossed shear sliding planes have occurred along the top of granular material under these loading and boundary conditions. These localized deformation patterns approximately agree with the experiment results under the parallel conditions^[3].

In this paper, adding a constant speed to the top plate, once the transverse strain exceeds the assembly's limit strain, the localized deformation will occur inside the granular material. We need some measurable parameters to reflect localized deformation inside the granular material. It is obvious that the localized deformation of granular material must result in variance of counterforce on the top plate from the granular material. This force can translate into the averaged stress on the top loading plate using the statistical averaged method. So it is convenient to reflect the localized deformation of granular material indirectly through the variance of the averaged stress acted on the top loading plate. Here we can define the predicted parameter η is the ratio of the averaged stress acted on the top loading plate to the confining pressure acted on the granular assembly laterally as follows:

$$\eta = \frac{\sigma_v}{\sigma_c}, \quad (9)$$

where σ_v is the averaged stress acted on the top loading plate, and σ_c is the lateral confining pressure. Figure 5 shows the relationships between the stress ratio η and the transverse strain ε . It can be found that the stress ratio increases up to the corresponding peak and then begins to drop with the increasing transverse strain. The decrease of the stress ratio indicates the reduction of load carrying capability which is caused by the localized deformation inside granular assembly. These localized deformations evolve into the shear sliding planes gradually. The limit strain is a limit state of the transverse strain before the shear planes occur and exactly correspond to the peak value of stress ratio. Before this point, the granular material is in the hardening stage, and when exceeding this point it gets in the softening stage and the localized deformation occurs. The similar phenomenon is also observed by experiments^[3]. Figure 6 shows a schematic diagram of all tangential

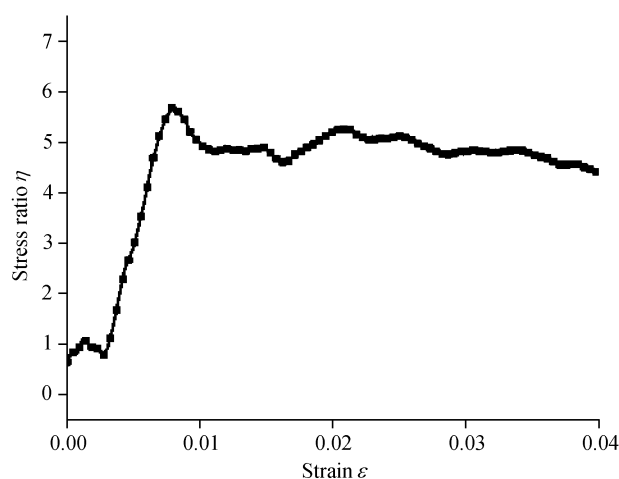


Figure 5 Stress ratios versus the transverse strains.

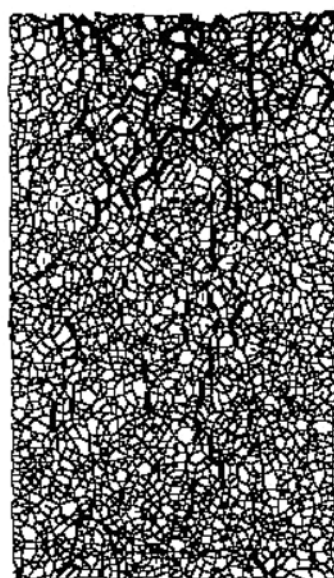


Figure 6 Tangential contact forces between particles.

forces between particles in granular assembly ($\varepsilon=0.017$). The direction and magnitude of tangential contact forces between particles are shown by force chains. It was found that tangential contact forces become larger distinctly around shear planes. However, this phenomenon was not found from normal contact forces between particles. This result shows that tangential contact forces play an important role in localized deformation of granular material.

Now we can analyze the characteristics of localized deformation and shear sliding planes. Figure 7 shows the schematic diagram of two shear planes in the reference model. Because the macro-shear planes in granular material are controlled by the micro-particle motions, we can use individual particle motions to define the characteristics of macro-shear planes, such as shear plane inclination angle. In this paper, the inclination angles of shear sliding planes are defined as the averaged value of angles between some particle motion directions and the horizontal direction. These particles can be selected to satisfy some restrictions, for example, the particle velocities in one direction exceed the median value of all particle velocities in this direction. In this paper, the inclination angle of shear sliding plane is defined as follows:

$$\theta = \frac{1}{N_c} \sum_{i=1}^{N_c} w_{ci} \theta_{ci} \quad (10)$$

where θ_{ci} is the angle between the particle motion direction and the horizontal direction, w_{ci} the weight value corresponding to θ_{ci} which reflects the influence of different particle velocity on the whole inclination angle of shear sliding planes, and N_c is the number of particles which satisfy the given restrictions. After two inclination angles of the shear sliding planes are defined, we can analyze their geometrical characteristics and evolving patterns with various external factors.

According to the definition of the inclination angle, we can decompose the velocity vectors along tangential directions of the two shear sliding planes. Figure 8 is the typical decomposed results ($D=2$ mm, $\varepsilon=0.017$). It can be seen obviously that two shear sliding planes occurred at this strain stage.

In order to analyze the shear sliding planes in detail, we divide the granular assembly into many sub-regions along the normal direction of shear sliding plane and calculate the corresponding averaged tangential velocities in each sub-region, and then we can get the shear velocity profile along the direction normal to the shear sliding planes. Figure 9 shows the evolving characteristics of two velocity profiles at different strain stages, where y_1 and y_2 are the local coordinates normal to the two shear sliding planes. From the figures we can find two different shear deformation modes. In the first shear mode illustrated in Figure 9(a), shear velocities decay very fast from the boundary in a near-exponential fashion along the direction normal to the first shear plane. In the second shear mode illustrated in Figure 9(b), the shear velocities decay in a near-linear fashion except for a little part near the boundary, indicating that it is a diffuse shear mode. In this mode, we can find transient shear bands at some conditions. Aharanov et al. have also observed two different shear modes from 2D numerical simulation of the plane shear granular layers^[19]. One is the fluid-like shear mode

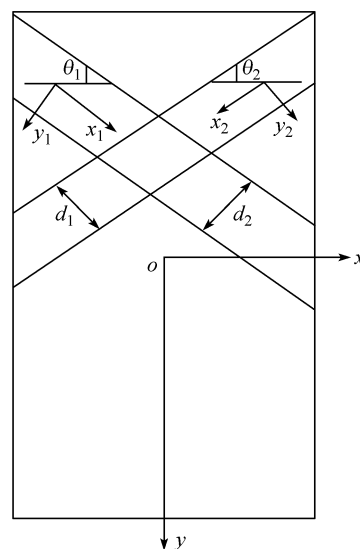


Figure 7 Schematic diagram of two shear planes.

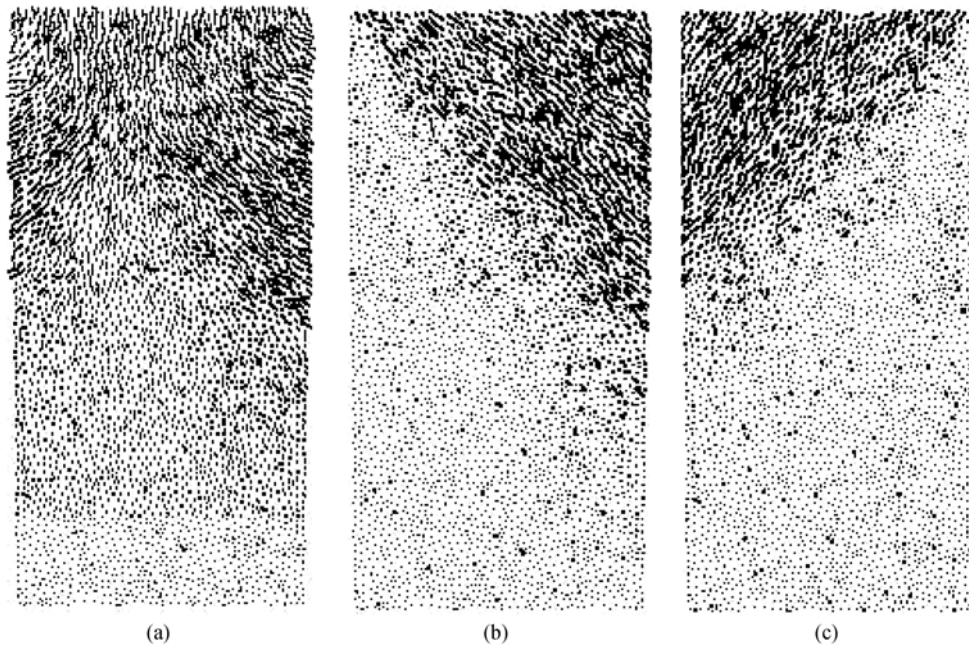


Figure 8 Decomposing process of whole deformation along two shear planes. (a) Velocity vector diagram of whole deformation; (b) velocity vector diagram along the first shear plane; (c) velocity vector diagram along the second shear plane.

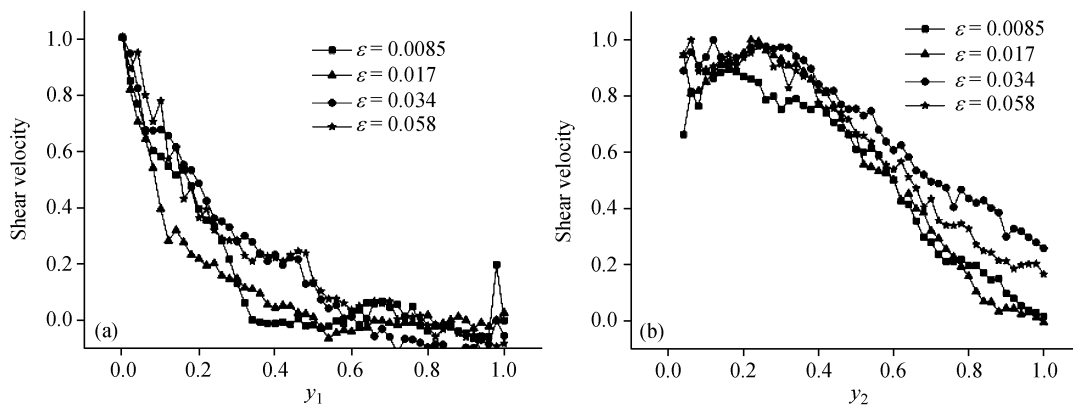


Figure 9 Shear velocity profiles along the normal direction of shear sliding planes at different strain stages. (a) The fluid-like shear mode; (b) the solid-like shear mode.

(mode F) whose velocity decays from the boundary in a near-exponential fashion, and another is the solid-like shear mode (Mode S) whose velocity decays from the boundary in a near-linear fashion. Through some numerical results we can find: (1) under plane strain conditions, two kinds of localized deformation modes (mode F and mode S) occur inside granular material. Different from the plane shear granular layers, these two kinds of localized deformation modes occur inside granular material simultaneously. (2) In the whole process of loading, two kinds of deformation modes may persist for a long time respectively. From simulating results, we also can find that the fluid-like shear mode is dominant in two kinds of shear modes. On one hand, we can find that the inclination angle corresponding to the fluid-like deformation mode is bigger than the inclination angle corresponding to the solid-like deformation mode. On the other hand, once the localized

deformation of granular material occurs, the fluid-like shear plane may occur and has always been accompanied by the whole deformation process when the shear mode evolves between the single-shear plane mode and the two-shear plane mode.

3.3 Influence of various material parameters and factors on the localized deformation

(i) Influence of initial void ratio. By changing the initial void ratio in the reference model, we can investigate the influence of this parameter on the localized deformation of granular material. Figure 10 shows the variation of stress ratio with the increase of transverse strain. From this figure, it can be found that the transverse strains corresponding to the peak points of stress ratio decrease as the initial void ratio decreases, but the peak value of stress ratio increases relatively. This phenomenon indicates that if the granular assembly is denser initially, the localized deformation in granular material may occur earlier but the granular assembly has a higher load bearing capacity under the same transverse strain. These results are in qualitative agreement with the experimental results^[3]. This can be easily understood: a higher initial void leaves more room for the whole compressive strain. There is a larger volumetric strain at the beginning stage of deformation. The localized deformation in granular material may occur when the void ratio reached a limit value. It can be found from the numerical testing that the limit value of void ratio is almost invariable under the same confining conditions. Therefore, the transverse strain corresponding to the occurrence of localized deformation will increase as the initial void ratio increases.

Figure 11 gives out inclination angles of the shear planes in granular material at different initial void ratios. It can be found that inclination angles of the shear planes are smaller for denser granular materials. We also can find that the first inclination angle corresponding to the fluid-like deformation mode is bigger than the second inclination angle corresponding to the solid-like deformation mode. These results are also in qualitative agreement with the experimental results^[3].

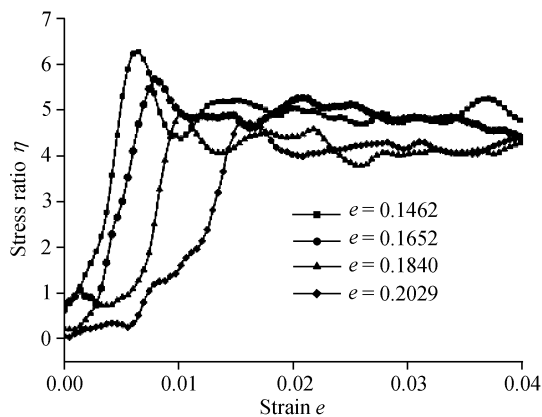


Figure 10 Influence of initial void ratio on stress ratio.

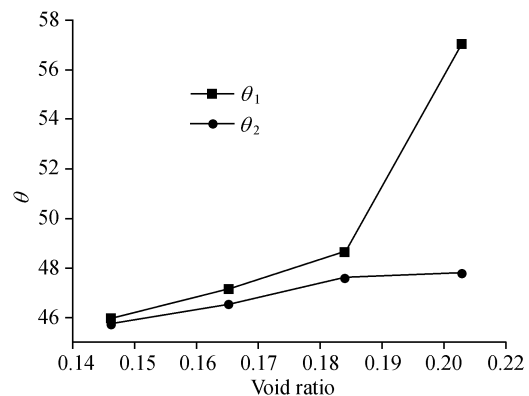


Figure 11 Effect of initial void ratio on inclination angles.

(ii) Influence of confining pressure. The cohesive force is not considered in this paper, so it is necessary to add lateral confining pressure to keep the initial stability of granular material. Commonly, confining pressure has strong influence on the localized deformation characteristics and the whole stabilities of granular material. Here we can directly use the stress added on the top loading plate as the predicted parameter to analyze the influence of confining pressure on stability of granular material. Figure 12 shows the influence of confining pressure on stress added on the top loading plate with the variance of transverse strain. From the figure, we can find that the stress peak

becomes higher as the confining pressure increases. This result indicates that the load carrying capability of granular material increases as the confining pressure increases.

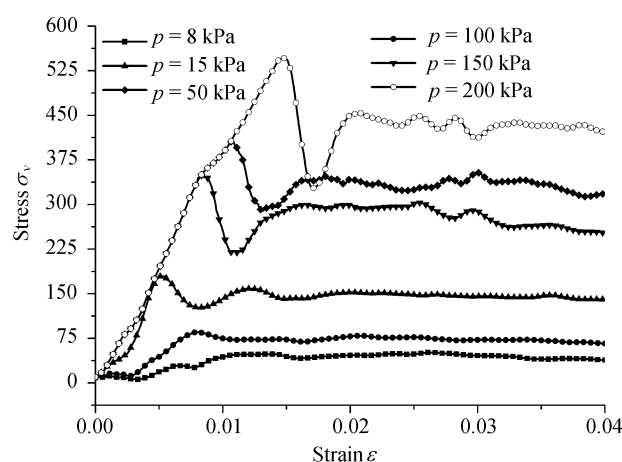


Figure 12 Influence of confining pressure on stress.

From the figure, we can also find that when confining pressure $\sigma_c \geq 50$ kPa, both the stress peak and the transverse strain corresponding to stress peak increase as confining pressure increases. This phenomenon shows that granular material has a whole compressive process if the confining pressure is high enough. In this process, localized deformation does not occur until the transverse strain exceeds its limit value. These results reflect that the limit value of transverse strain increases as the confining pressure increases, leading to higher stability of granular material. If confining pressure $\sigma_c \leq 15$ kPa, the occurrence of stress peak is not clear in the figure. This phenomenon can be explained through numerical simulations that granular material has whole horizontal diffusion during the loading process if the confining pressure is small. This whole horizontal diffusion may result in the increase of the limit value of transverse strain. If the confining pressure is too small, no clear localized deformation and shear plane are observed inside granular material. This conclusion has been observed in former simulation results reported by Iwashita et al.^[10]. Through the simulation results, we can also find that with the increase of the confining pressure, the solid-like shear pattern is weakening and the crossing shear planes gradually evolve into the single shear plane.

(iii) Influence of the friction coefficient. This section will demonstrate that the friction coefficient affects significantly the mechanism of localized deformation in granular material. Through the results of numerical simulation, we can obtain some interesting conclusions. When the friction coefficient μ equals zero, some annular motion clusters have occurred inside granular material because friction forces between individual particles disappear, and we cannot find clear shear sliding planes inside granular material during the whole loading process. With the increase of friction coefficient, a distinct shear sliding plane gradually occurs inside the granular assembly as shown in Figure 13. From the figure, it can be found that when the friction coefficient μ is small, there is only one distinct shear plane inside the granular material. Using the tangential velocity profile along the normal direction of shear plane, we can find this shear sliding plane belongs to a fluid-like shear pattern. With the increase of the friction coefficient μ , the solid-like shear sliding plane appears gradually, and then the single shear plane evolves into two different shear planes. In contrast to the single-shear pattern, the two-shear pattern usually leads to a higher load bearing

capacity. So the whole stability of granular assembly will gradually strengthen with the increase of friction coefficient.

Figure 14 gives the influence of friction coefficient on stress ratio. From the figure, we can find that the stress ratio curves fluctuate intensely when friction coefficient μ is small. This period accompanies the strain hardening process and the softening process, and the stability of granular assembly is poor. As friction coefficient μ increases, the fluctuations of stress ratio curves reduce and the load carrying capability of granular material increases. When friction coefficient μ is small, only a single fluid-like shear plane is observed inside the granular material, and inclination angle of this shear plane increases slightly with the increase of friction coefficient illustrated in Figure 15.

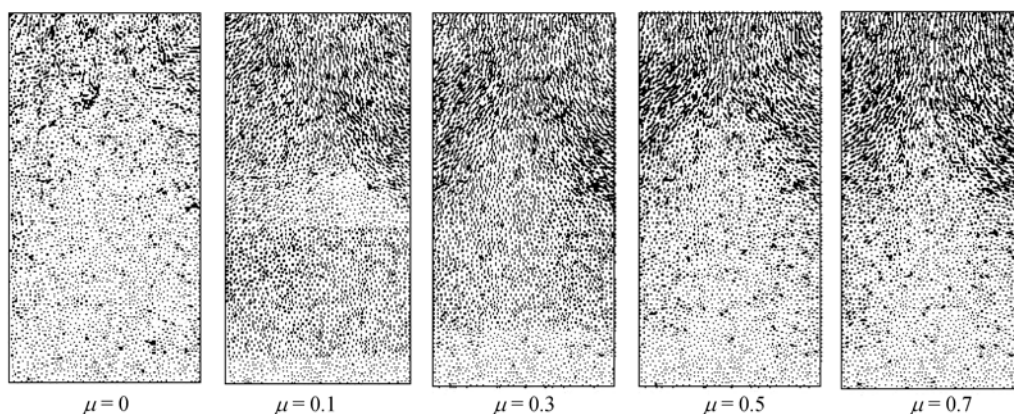


Figure 13 Velocity vectors with different friction coefficients.

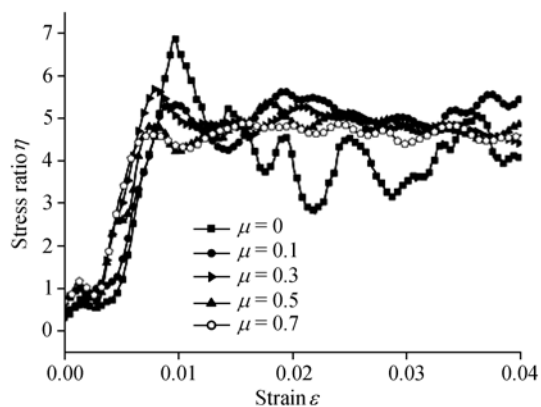


Figure 14 Influence of friction coefficient on stress ratio.

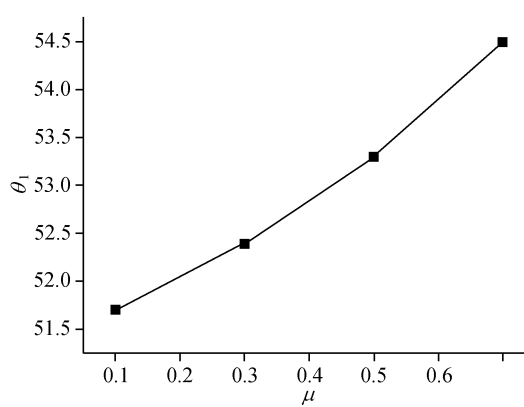


Figure 15 Influence of friction coefficient on inclination angle.

4 Conclusions

In this paper, we analyze the features and developments of the localized deformation in stochastic distributed granular materials under the plane strain conditions using MDEM. The influences of various material parameters or factors on the localized deformation features and patterns, stability, inclinations of shear sliding planes in the granular materials are also discussed in detail. Conclusions are given as follows:

- (1) Two crossed shear sliding planes inside the stochastic distributed granular material can occur

under the plane strain loading conditions.

(2) The shear velocity profiles along the normal direction of the two shear sliding planes are different completely, one is fluid-like shear deformation pattern, and the other is solid-like shear deformation pattern. In the whole process of loading, two kinds of deformation modes may persist for a long time respectively. During the whole compression process, the fluid-like shear mode is dominant in two kinds of modes.

(3) The initial void ratio has influences on the localized deformation of granular material. If the granular material is denser initially, localized deformations in granular material may occur earlier but the granular assembly has a higher load bearing capacity under the same transverse strain. Inclination angles of shear planes increase as the initial void ratio increases.

(4) Confining pressure also has strong influence on the localized deformation patterns and the whole stabilities of granular material. With the increase of confining pressure, load carrying capability of the granular material increases and the limit value of transverse strain also increases. From the simulation testing, it can also be found that the solid-like shear pattern is weakening and two crossing shear planes gradually evolve into the single shear plane.

(5) When friction coefficient is small, only a single fluid-like shear plane is observed inside the granular material. With the increase of friction coefficient, the solid-like shear sliding plane appears gradually, and then one shear plane evolves into two different shear planes gradually.

- 1 Tordesillas A, Walsh D C D. Incorporating rolling resistance and contact anisotropy in micromechanical models of granular media. *Powder Technol*, 2002, 124: 106–111
- 2 Kuhn M R. Structured deformation in granular materials. *Mech Mater*, 1999, 31: 407–429
- 3 Khalid A A, Stein S. Shear band formation in plane strain experiments of sand. *J Geotech Geoenviron*, 2000, 126(6): 495–503
- 4 Labuz J F, Dai S T. Residual strength and fracture energy from plain-strain testing. *J Geotech Geoenviron*, 2000, 126(10): 882–889
- 5 Wang Q, Lade P V. Shear banding in true triaxial tests and its effect on failure in sand. *J Eng Mech*, 2001, 127(8): 754–761
- 6 Nübel K, Huang W X. A study of localized deformation pattern in granular media. *Comput Meth Appl Mech Engrg*, 2004, 193: 2719–2743
- 7 Tejchman J. Influence of a characteristic length on shear zone formation in hypoplasticity with different enhancements. *Comput Geotech*, 2004, 31: 595–611
- 8 Gardiner B S, Tordesillas A. Micromechanics of shear bands. *Int J Solids Struct*, 2004, 41: 5885–5901
- 9 Iwashita K, Oda M. Rolling resistance at contacts in simulation of shear band development by DEM. *J Eng Mech*, 1998, 124(3): 285–292
- 10 Iwashita K, Oda M. Micro-deformation mechanics of shear banding process based on modified distinct element method. *Powder Technol*, 2000, 109: 192–205
- 11 Jiang M J, Yu H S, Harris D. A novel discrete model for granular material incorporating rolling resistance. *Comput Geotech*, 2005, 32: 340–357
- 12 Hu N, Molinari J F. Shear bands in dense metallic granular materials. *J Mech Phys Solids*, 2004, 52: 499–531
- 13 Cundall P A, Strack O D L. A discrete numerical model for granular assemblies. *Geotechnique*, 1979, 29(1): 47–65
- 14 Zhu H P, Yu A B. A theoretical analysis of the force models in discrete element method. *Powder Technol*, 2006, 161: 122–129
- 15 Nezami E G, Hashash Y M. A fast contact detection algorithm for 3-D discrete element method. *Comput Geotech*, 2004, 31: 575–587
- 16 Hsiao S S, Yang S C. Numerical simulation of self-diffusion and mixing in a vibrated granular bed with the cohesive effect of liquid bridges. *Chem Eng Sci*, 2003, 58: 339–351
- 17 Bertrand F, Leclaire L A, Levecque G. DEM-based models for the mixing of granular materials. *Chem Eng Sci*, 2005, 60: 2517–2531
- 18 Aharanov E, Sparks D W. Rigidity phase transition in granular packing. *Phys Rev E*, 1999, 60: 6890–6896
- 19 Aharanov E, Sparks D W. Shear profiles and localization in simulations of granular materials. *Phys Rev E*, 2002, 65(5): 051302-1–12